DOI 10.1002/pmic.200401095 *Proteomics* 2005, *5,* 2010–2017

REGULAR ARTICLE

Peptide microarrays for the detection of molecular interactions in cellular signal transduction

Oda Stoevesandt[1], Martin Elbs[1]*#, Karsten Köhler[1], Annemarie C. Lellouch[2], Rainer Fischer[1], Thomas André[1] and Roland Brock[1]*

[1] Institute for Cell Biology, University of Tübingen, Tübingen, Germany
[2] Centre d'Immunologie de Marseille-Luminy, CNRS-INSERM-Université de la Mediterranée, Marseille, France

The formation of protein complexes is a hallmark of cellular signal transduction. Here, we show that peptide microarrays provide a robust and quantitative means to detect signalling-dependent changes of molecular interactions. Recruitment of a protein into a complex upon stimulation of a cell leads to the masking of an otherwise exposed binding site. In cell lysates this masking can be detected by reduced binding to a microarray carrying a peptide that corresponds to the binding motif of the respective interaction domain. The method is exemplified for the lymphocyte-specific tyrosine kinase 70 kDa zeta-associated protein binding to a bis-phosphotyrosine-motif of the activated T-cell receptor *via* its tandem SH2 domain. Compared to established techniques, the method provides a significant shortcut to the detection of molecular interactions.

Received: March 18, 2004
Revised: August 30, 2004
Accepted: October 28, 2004

Keywords:
Cellular immunity / Fluorescence correlation spectroscopy / Signal transduction domain

1 Introduction

Over the past years, oligonucleotide microarrays have revolutionised the way in which changes in gene expression can be detected in parallel [1–4]. Recently, similar advances in the measurement of protein levels have been achieved using antibody arrays [5]. The changes in mRNA and protein content detected by these types of arrays are the result of signal transduction processes. Given the complexity of signalling networks, the application of microarrays for the parallel analysis of signal transduction events seems evident. However, except for microarray sensing kinase activities [6], the molecular events constituting these signalling processes have so far largely escaped detection by microarrays. Especially for the parallel detection of molecular interactions, conceptual advances are required.

We realised that microarrays of peptides corresponding to protein interaction motifs [7] may provide a specific means for detecting the signalling-dependent masking or unmasking of binding sites. If, inside a cell, a protein engages in a molecular interaction, the binding domain involved in this interaction is masked. Complex formation should therefore decrease the amount of protein available for binding to the microarray after lysis (Fig. 1). Peptide arrays have been employed already to profile the structural requirements of the binding of protein domains [8, 9]. For interaction motifs involving PTMs, such as phosphorylation, peptide microarrays are advantageous compared to protein microarrays.

Correspondence: Dr. Roland Brock, Institute for Cell Biology, University of Tübingen, Auf der Morgenstelle 15, 72076 Tübingen, Germany
E-mail: roland.brock@uni-tuebingen.de
Fax: +49-7071-29-5891

Abbreviations: FCS, fluorescence correlation spectroscopy; **Fluo**, 5(6)-carboxyfluorescein; **ITAM**, immunoreceptor tyrosine-based activation motif; **TPBS**, PBS with 0.05% Tween-20; **TCR**, T-cell receptor; **YFP**, enhanced yellow fluorescent protein; **ZAP-70**, 70 kDa zeta-associated protein

* These authors contributed equally to this work.
\# Current address: Department of Chemistry, UCL, 20 Gordon Street, London WC1H 0AJ, UK

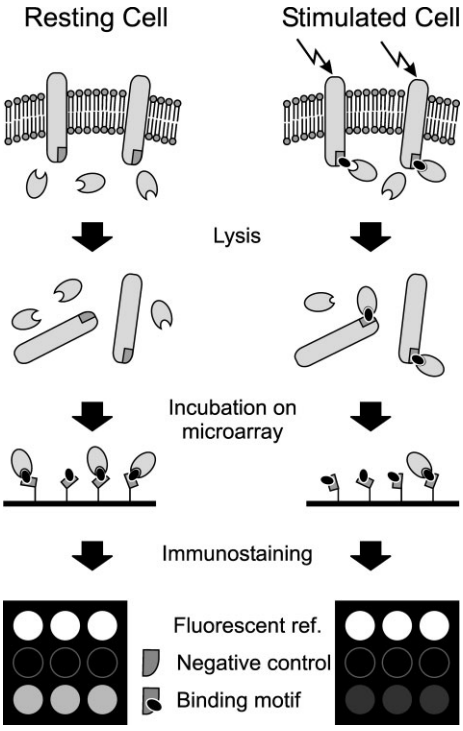

Figure 1. Schematic of the application of peptide microarrays for detecting the masking of binding sites. Peptide microarrays are generated from peptides that correspond to motifs interacting with binding domains of signalling proteins. Recruitment of a protein into a complex masks a binding site on the protein, which is therefore no longer available for interaction with the microarray. Consequently, those proteins engaging in a molecular interaction will yield weakened signals on the microarray. The binding of proteins may be detected in parallel by immunofluorescence, employing cocktails of primary antibodies. The pattern of proteins bound to the microarray reflects the pattern of molecular interactions inside the cells.

Amino acids carrying PTMs can be incorporated in a site-specific manner by organic synthesis procedures. For the detection of protein-peptide interactions, purified recombinant proteins as well as crude cell lysates [10] have served as the source for protein.

In order to validate our concept, the activation dependent interaction of the tyrosine kinase 70 kDa ζ-associated protein (ZAP-70) with the T-cell receptor (TCR)-associated CD3ζ-chain, was selected as a model system [11]. ZAP-70 consists of an *N*-terminal tandem SH2 domain and a *C*-terminal tyrosine kinase domain. In resting cells, this protein distributed is throughout the cell [12]. Crosslinking of the TCRs by MHC-peptide complexes on an antigen-presenting cell leads to the phosphorylation of several tyrosine residues within immunoreceptor tyrosine-based activation motifs (ITAM) of the CD3ζ-chain [13]. The bis-phosphorylated CD3ζ ITAM peptide motif NQL(pY)NELNLGRREE(pY)DVL acts as a high-affinity docking site for the tandem SH2 domain of ZAP-70 and recruits ZAP-70 to the plasma membrane. Using plasmon resonance spectroscopy, an apparent dissociation constant of 2.0 ± 0.5 nM was reported for this interaction [14]. Once incorporated into the TCR complex, ZAP-70 becomes phosphorylated and fully activated and initiates a series of downstream signalling events [15].

In the experiments presented here, peptide microarrays were functionalised with the bis-phosphorylated CD3ζ ITAM (pITAM) peptide and the nonphosphorylated counterpart (ITAM). Lysates of cells overexpressing a fusion protein of ZAP-70 with the enhanced yellow fluorescent protein (ZAP-70-YFP) and of cells expressing endogenous amounts of ZAP-70 were used as the source for the protein. Binding of ZAP-70 to the microarray was either detected by virtue of the intrinsic fluorescence of the fusion protein or by indirect immunofluorescence. In both cases, the activation-dependent recruitment of ZAP-70 into signalling complexes reduced the microarray-bound signal. This reduction in signal provides quantitative information on the change of the fraction of available binding sites and even on the number of available binding sites *per* cell.

2 Materials and methods

2.1 Peptides

The phosphopeptide C-Ahx-NQL(pY)NELNLGRREE(pY)DVL-NH_2 (pITAM), the nonphosphorylated control peptide Ac-C-Ahx-NQLYNELNLGRREEYDVL-NH_2 (ITAM) and the fluorescein-labelled control peptide Fluo-Ahx-KAA were synthesised as described in the supplementary material section.

2.2 Generation of microarrays

The preparation of microarrays followed a protocol described previously [16]. In brief, coverslips (BK7, type 1 with 12 mm diameter) were cleaned by sonication in an aqueous solution of Extran MA01 (Merck, Darmstadt, Germany)/water (1:4, v/v) for 5 min followed by sonication in piranha solution, a freshly prepared mixture of H_2SO_4/30% v/v H_2O_2 (6:5, v/v) for 20 min. For silanisation coverslips were covered with 40 μL of (3-glycidyloxypropyl)trimethoxysilane (Fluka, Deisenhofen, Germany), placed in an airtight container and incubated at room temperature for 6 h, followed by rinsing with acetone. Immediately after silanisation the dry coverslips were functionalised with the peptides. Peptides were dissolved to a concentration of 100 μM in 100 mM phosphate buffer (pH 8.0). Peptide solutions (0.8 nL) were spotted with a GeSiM NP2.0 nanopipettor (GeSiM, Dresden, Germany) with a centre-to-centre spacing of 300 μm, maintaining 80% humidity within the spotter casing. After 30 min at room temperature, the coverslips were dried and incubated with 80 μL of *O,O'*-bis(2-aminopropyl)PEG 800 (Fluka) at 70°C for 16 h to quench the remaining reactive groups. After cooling, the coverslips were rinsed with water, dried under an airstream and stored at room temperature.

2.3 Cell culture and preparation of cell lysates

3A9 T-hybridoma cells and derivatives transfected with both ZAP-70-YFP and a fusion protein of the CD3ζ-chain with cyan fluorescent protein (CFP), or both free YFP and CD3ζ-CFP were cultured in DMEM supplemented with 10% fetal calf serum, 100 μM sodium pyruvate, nonessential amino acids and 200 μM L-glutamine. The generation of the transfected cell lines is described in the supplementary material section. The broad-range phosphatase inhibitor sodium pervanadate was generated in a freshly prepared mixture of 5 mM Na_3VO_4 and 5 mM H_2O_2 in HEPES-buffered saline (HBS; 10 mM HEPES, 135 mM NaCl, 5 mM KCl, 1 mM $MgCl_2$, 1.8 mM $CaCl_2$, pH 7.4). The solution was incubated at room temperature for 15 min and used immediately at a tenfold dilution. For activation, cells suspended in HBS supplemented with 0.1% BSA and 5 mM glucose were incubated with pervanadate for 20 min at 37°C. Cell lysates were prepared by suspension of cells in lysis buffer (1% Triton X-100, 20 mM Tris, 1 mM EDTA, 150 mM NaCl, protease inhibitor cocktail (Roche, Mannheim, Germany), 1 mM Na_3VO_4, pH 7.5). Unless indicated otherwise, 10^7 cells *per* 1 mL of lysis buffer were used. After lysis on ice for 30 min, the crude lysates were clarified by centrifugation at 20 000 × *g* for 15 min. Total protein concentration of lysates was determined by a standard protein assay (Bio-Rad, Munich, Germany).

2.4 SDS-PAGE and Western blotting

SDS-PAGE of lysates was carried out according to the procedure described by Laemmli [17]. The gel was blotted on a PVDF membrane (Millipore, Schwalbach, Germany) using 25 mM Tris, 192 mM glycine, 20% v/v methanol (pH 8.3) as transfer buffer. After blocking with 5% nonfat dry milk powder in TPBS (PBS, 0.05% Tween-20), the blot was developed using a mouse mAb directed against a *C*-terminal part of ZAP-70 (BD Transduction Laboratories, Franklin Lakes, USA), an alkaline phosphatase-conjugated anti-mouse IgG secondary antibody (Sigma, Munich, Germany) and a colorigenic substrate. Western bands were quantified by scanning the blots and integrating mean signal intensity and area of the bands.

2.5 Microscopy

Confocal laser scanning microscopy was performed using an inverted LSM510 confocal laser scanning microscope (Carl Zeiss, Göttingen, Germany). YFP was excited with the 514 nm line of an argon-ion laser and detected using a BP530–600 nm band pass filter, Cy5 was excited with the 633 nm line of a helium neon laser and detected using an LP650 nm long pass filter. Cell images were acquired at a sampling rate of 1024 × 1024 pixels using a C-Apochromat 63 × 1.2 NA water immersion objective. The coverslips with the arrayed peptides were mounted in a custom-made open measurement chamber with the coated surface up, allowing addition of solution to the microarray during observation. One hundred microlitres of cell lysate or antibody solutions were used for incubation on each coverslip. After addition to the coverslip, the solution was mixed by pipetting up and down several times. Incubation was carried out for 3 min for the lysates and 15 min for antibodies. Antibodies were diluted to 5 μg/mL for anti-ZAP-70, to 15 μg/mL for anti-phosphotyrosine (Cell Signaling Technologies, Beverly, USA) and to 2.8 μg/mL for Cy5-labelled goat-anti-mouse-antibody (Dianova, Hamburg, Germany) in TPBS containing 0.5% BSA. Between each incubation step, arrays were washed twice with TPBS. Digital images were acquired at a sampling rate of 512 × 512 pixels using a Plan-Neofluar 10 × 0.3 NA objective. For data evaluation, the functionalised spots and the surrounding background were defined as separate areas of interest and the mean intensity within the respective area of interest determined using Image Pro Plus 4.5 for Windows 2000 (Media Cybernetics, Silver Spring, USA). The net fluorescence (F) was calculated by subtracting the mean intensity of the background from the mean intensity of the respective spot. The net fluorescence over equally functionalised spots was averaged.

2.6 Fluorescence correlation spectroscopy (FCS)

FCS measurements in cell lysates were performed using a ConfoCor2 fluorescence correlation spectroscope (Carl Zeiss). YFP was excited with the 514 nm line of an argon-ion laser and detected using an infrared-blocking BP535–590 nm bandpass filter. For each condition, 10 FCS measurements of 15 s duration each were recorded. Autocorrelation functions were calculated online and the data were evaluated using the LSM-FCS software (V. 2.8; Carl Zeiss). YFP autocorrelation curves were fitted between 10 μs and 1 s (Eq. 1).

$$G(\tau) = 1 + \frac{1}{N} \cdot \frac{1}{1 + \left(\tau/\tau_D\right)} \cdot \frac{1}{\sqrt{1 + \tau/S^2 \cdot \tau_D}} \cdot \left(1 + \frac{R}{1-R} \cdot e^{-\frac{\tau}{\tau_R}}\right) \quad (1)$$

The fit formalism accounted for one species of fluorescent particles with a diffusional autocorrelation time τ_D and an average number of particles *N* in the detection volume, and protonation-dependent fluctuations in YFP fluorescence with a relaxation time τ_R and a fraction *R* of molecules in the protonated state [18]. $S = z_0/\omega_0$ denotes the instrument-specific structure parameter, where z_0 and ω_0 are the radii of the detection volume along the optical axis and in the optical plane, defined by the isocontour of e^{-2} detection efficiency relative to the centre of the confocal detection volume. Molar concentrations of ZAP-70-YFP were calculated from the numbers of particles *N* present in the confocal detection volume V_{det} according to Eq. 2:

$$c = \frac{N}{N_A V_{det}} = \frac{N}{N_A \pi^{3/2} \omega_0^3 S} = \frac{N}{N_A S (4\pi D_{cal} \tau_{D,cal})^{3/2}} \quad (2)$$

N_A is Avogadro's constant. The structure factor S and the diffusional autocorrelation time $\tau_{D,cal}$ were determined in a calibration measurement using carboxyrhodamine 6G (Molecular Probes, Leiden, The Netherlands) with the known diffusion coefficient $D_{cal} = 2.8 \times 10^{-6}$ cm^2/s.

3 Results and discussion

In T-cell signal transduction the bis-phosphorylated pITAM preferentially interacts with the tandem SH2 domain of the ZAP-70 tyrosine kinase [14, 19]. Because of its relevance for the propagation of the TCR signal, this peptide motif was selected to probe for the masking of signalling domains using a peptide microarray approach (Fig. 1). The non-phosphorylated counterpart (ITAM) served as a control for the specificity of binding. Both peptides were synthesised as peptide amides with an *N*-terminal cysteine residue for the covalent immobilisation on epoxy-activated surfaces. Ahx served as a spacer. Fluo-Ahx-KAA was employed as a control for surface chemistry and spotting. This peptide was immobilised *via* the ε-amino group of the lysine side-chain. Microarrays were generated by nanopipetting subnanolitre volumes of solutions of the peptides.

In initial experiments, ZAP-70-containing cell lysates were prepared from cells stably overexpressing a ZAP-70-YFP fusion protein as well as a fusion protein of the ZAP-70-binding CD3ζ-chain with the CFP (CD3ζ-CFP). Binding of the ZAP-70 fusion protein to the microarray was detected using a confocal microscope by recording the YFP fluorescence or after indirect immunofluorescence staining.

For microarrays incubated with lysis buffer, only the fluorescence of the fluorescein-labelled control peptide could be detected (Fig. 2A). When microarrays were incubated with lysate from resting cells expressing ZAP-70-YFP, the pITAM spots showed a bright fluorescence, indicating an interaction of the peptide with the ZAP-70 tandem SH2 domains, whereas the ITAM spots remained dark (Fig. 2B). The specificity of the binding of ZAP-70-YFP to the pITAM was further confirmed by preincubation of the lysate with 1 μM of free pITAM peptide to block available SH2 domains. Here, only the reference spots were visible (not shown).

In comparison to lysates of resting cells, for lysates of cells treated with the tyrosine phosphatase inhibitor sodium pervanadate, binding of ZAP-70-YFP was strongly reduced (Fig. 2C). The pITAM-associated net fluorescence was only about one-quarter to one-third of that detected for lysates of resting cells (graph in Fig. 2). Inhibition of tyrosine phosphatases leads to a strong phosphorylation of the transmembrane protein CD3ζ by protein tyrosine kinases. On the whole-cell level the effect of pervanadate was apparent by the recruitment of ZAP-70-YFP to the plasma membrane

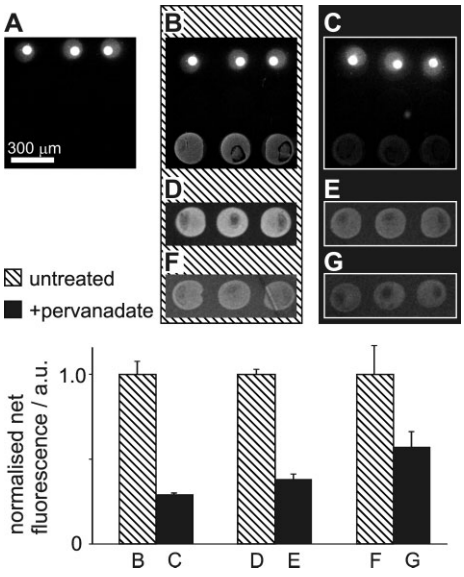

Figure 2. Activation-dependent binding of the ZAP-70 tyrosine kinase to peptide microarrays. All microarrays contained spots of a fluorescein labelled peptide, serving as a control for the surface chemistry (upper row in A–C), the unphosphorylated ITAM-peptide (middle row in A–C) and the bisphophorylated pITAM-peptide (lower row in A–C). (D–G) pITAM spots. Microarrays were scanned by confocal fluorescence microscopy. (A) Microarray incubated with lysis buffer. Microarrays in (B, D, F) were incubated with lysates of resting cells, those in (C, E, G) with corresponding lysates of cells treated with sodium pervanadate. (B, C) Binding of ZAP-70-YFP detected by YFP-fluorescence, (D, E) binding of ZAP-70-YFP after indirect immunostaining for ZAP-70 using Cy5-fluorescence. (F, G) Indirect immunostaining of endogenous ZAP-70. The image contrast of each set of images (A–C; D, E; F, G) was optimised separately. The graph depicts the mean intensity of the background-corrected fluorescence of each set of spots, normalised to the untreated condition for each experiment. Error bars reflect the mean deviation of the mean for each condition.

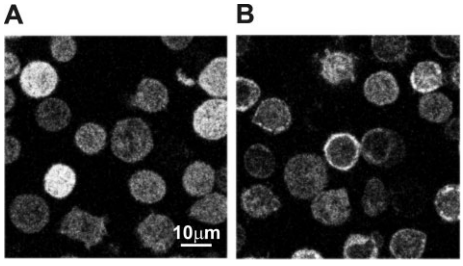

Figure 3. Pervanadate-dependent cellular redistribution of ZAP-70-YFP. In resting cells, ZAP-70-YFP was evenly distributed (A). After incubation with pervanadate, ZAP-70-YFP was recruited to the membrane-proximal region (B).

(Fig. 3). The observed decrease in the microarray-bound signal is therefore consistent with the activation-dependent masking of the ZAP-70 SH2 domains and reduction of protein available for binding. A comparable reduction in signal was also observed when ZAP-70-YFP binding was

detected by indirect immunofluorescence using an anti-ZAP-70 primary and a Cy5-labelled secondary antibody (Fig. 2D and E).

Up to this point, the microarrays had succeeded in detecting an activation-dependent reduction of protein binding using cells in which both binding partners were overexpressed. Western blot analysis revealed that the level of ZAP-70-YFP fusion protein was about 2.5 times the level of endogenous protein in nontransfected cells (Fig. 4A). In order to test whether the microarray approach was sensitive enough to detect the masking of binding sites in lysates of cells expressing endogenous amounts of both proteins, untransfected cells were employed. Binding of ZAP-70 could be detected by immunofluorescence. Again, pervanadate treatment led to a significant reduction in the signal (Figs. 2F and G).

To exclude a pervanadate-dependent degradation of total protein or specifically of ZAP-70 as the cause of the reduced binding, lysates of pervanadate treated and resting cells were analysed for protein content and ZAP-70 levels. Neither the total protein content (data not shown) nor the ZAP-70 content were influenced by pervanadate (Fig. 4A). FCS in lysates of ZAP-70-YFP expressing cells was employed to further substantiate that the reduction in binding reflected recruitment of ZAP-70 into molecular complexes. FCS derives information on diffusion constants of fluorescent particles by the analysis of temporal fluctuations of a fluorescence signal [20, 21]. In a close approximation, the diffusion constant of a particle is inversely related to the cubic root of its mass. The intrinsic fluorophore YFP allows the sensitive detection of fusion proteins by FCS. Autocorrelation functions of ZAP-70-YFP could be derived from fluorescence fluctuations recorded in crude cell lysates of pervanadate treated and resting cells. For pervanadate treated cells, the autocorrelation curve was shifted towards longer autocorrelation times. The observed shift corresponded to a decrease of the diffusion constant by 45% and a six-fold increase in mass of the fluorescent particle, consistent with the recruitment of ZAP-70-YFP into high-molecular weight complexes (Fig. 4B). No such change was observed for cells expressing free YFP instead of ZAP-70-YFP.

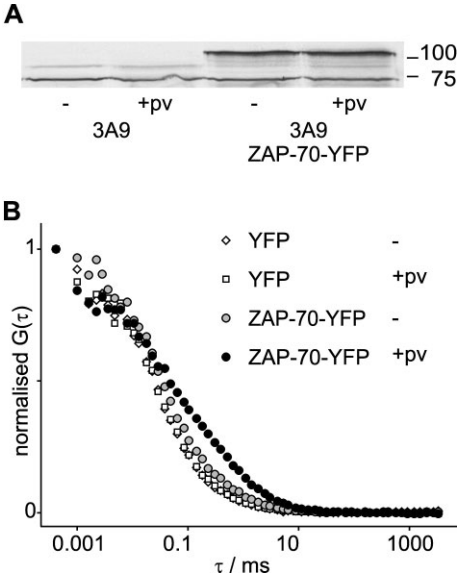

Figure 4. (A) Cellular content of ZAP-70 and ZAP-70-YFP before and after pervanadate treatment. Lysates of untransfected cells and cells overexpressing ZAP-70-YFP and CD3ζ-CFP, both treated with pervanadate or left untreated, were probed by Western blot analysis for ZAP-70. Equal amounts of protein were loaded in each lane. Endogenous ZAP-70 runs at an apparent molecular weight of 70 kDa, ZAP-70-YFP at approximately 100 kDa. (B) Validation of ZAP-70 complex formation upon pervanadate treatment by FCS. Autocorrelation functions were determined from lysates of cells overexpressing ZAP-70-YFP and CD3ζ-CFP, treated with pervanadate or left untreated. The amplitudes of the autocorrelation functions were normalised to unity. The decay time of the autocorrelation function reflects the size of the fluorescent particle. As a control, FCS measurements were performed in lysates of pervanadate treated or resting cells expressing free YFP.

Although a marked reduction of the pITAM-bound fluorescence was consistently found after pervanadate treatment, the reduction was stronger for cells overexpressing the fusion protein (Fig. 2). This observation could either be due to the fact that the transfected cells also overexpressed the CD3ζ-chain or inherent to the detection method, *i.e.*, YFP-fluorescence *versus* indirect immunofluorescence. In order to resolve this question, we next asked to which degree the changes in signal on the microarray correlated with the availability of binding sites of ZAP-70 in the cell lysate. Given such a correlation, microarray-based analyses would yield a quantitative measure of changes in molecular interactions in cellular signalling. In a first step, we took advantage of the ability of FCS to directly determine the concentration of fluorescent molecules. Lysates of resting cells expressing ZAP-70-YFP were prepared at different cell densities, ranging from 2 to 50 $\times$ 10^6 cells *per* millilitre lysate. The total protein content increased linearly with the cell density. The same was found for the ZAP-70-YFP concentration, determined by FCS. By autocorrelation analysis, concentrations of the fusion protein in the cell lysates between 4 and 85 nM were derived. Moreover, the net fluorescence of ZAP-70-YFP bound to pITAM spots on the microarrays was directly proportional to the concentration of ZAP-70-YFP in the examined range (Fig. 5A). This calibration curve provided the basis to determine the decrease in the concentration of available binding sites upon treatment with pervanadate. In a lysate of 1 $\times$ 10^7 resting cells *per* millilitre the concentration of ZAP-70-YFP was 19.9 $\pm >$ 2.2 nM. From the reduction of the array-bound fluorescence after pervanadate treatment, a reduction of unbound ZAP-70-YFP to 7.1 $\pm >$ 0.4 nM was calculated for a lysate of corresponding cell density (Fig. 5A). In order to confirm that the concentration determined by FCS corresponded to the concentration of ZAP-70-YFP with available binding sites, we performed an immunoprecipitation of the CD3ζ-chain (not shown). Only after pervanadate treat-

ment, ZAP-70 coprecipitated with the CD3ζ-chain. In resting cells, no interaction of ZAP-70 with the CD3ζ-chain was detectable.

At this point we were concerned, that the activation-dependent change in the level of microarray-bound ZAP-70 could also have arisen from a competition of ZAP-70 with other proteins in the lysate for which an activation-dependent unmasking of binding sites had occurred. Such a competition would take place if binding of protein to the peptide spots was close to saturation. The linear dependence of array-bound fluorescence and ZAP-70-YFP concentration to lysate densities of up to 5×10^7 cells *per* millilitre, five times the density employed for the quantification of activation-dependent changes, indicated that binding of ZAP-70 to the microarray was clearly below saturation. The capacity of the spots for binding protein was further analysed by detection of remaining free pITAM after incubation with lysate. Here we took advantage of the detectability of the pITAM peptide by indirect immunostaining, using antiphosphotyrosine primary and Cy5-labelled secondary antibodies. With increasing lysate concentration, Cy5-fluorescence decreased by half (Fig. 5B), demonstrating that the pITAM peptide was not a limiting factor for detecting activation-dependent changes in the masking of binding sites.

Next, we intended to demonstrate that for endogenous protein as well, calibration curves can provide quantitative information on the masking of binding sites. Lysates of untransfected resting cells were prepared at cell densities up to 5×10^7 *per* millilitre lysate. The ZAP-70 content of the lysates as determined by Western blot analysis scaled linearly with the cell density (Fig. 5C and D). Again, the microarray-bound fluorescence after indirect immunostaining correlated positively with the ZAP-70 content. In contrast to the fluorescence of the ZAP-70-YFP fusion protein, the correlation was nonlinear (Fig. 5E). In the lysates of cells expressing ZAP-70-YFP, the fusion protein was overexpressed by 2.5-fold in addition to the endogenous protein (Fig. 4A) and the arrays were still not saturated at the highest lysate concentration tested. Therefore, the nonlinear increase of immuno-

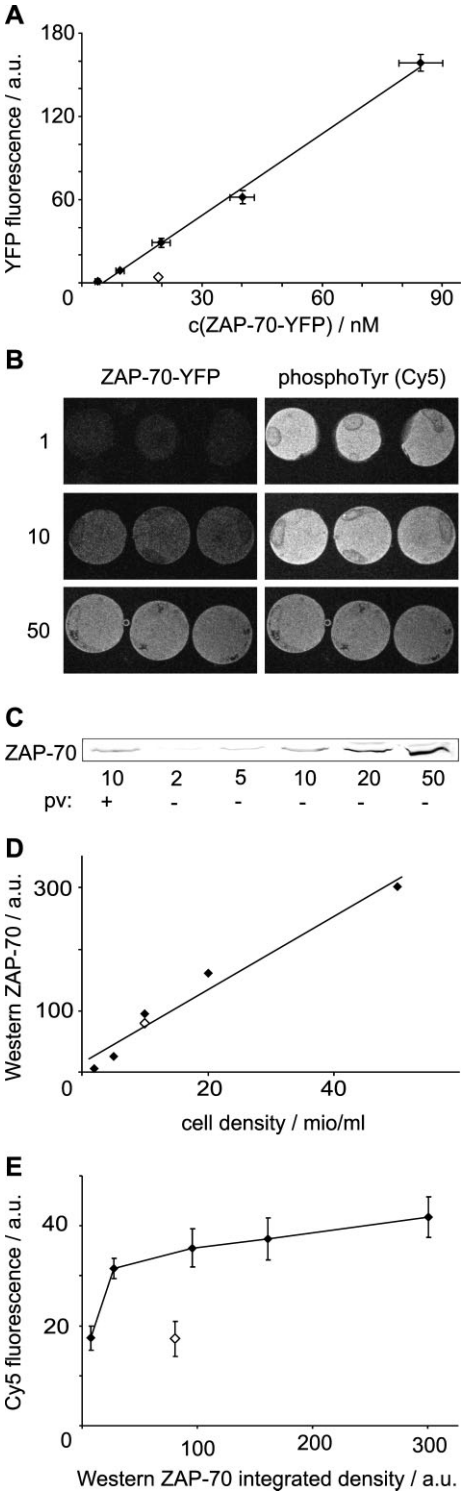

Figure 5. Relation between the concentration of ZAP-70 in the lysates of resting cells and array-bound fluorescence on pITAM spots after incubation on microarrays. (A) Lysates of resting cells expressing ZAP-70-YFP were prepared at cell densities of 2, 5, 10, 20 and 50×10^6 cells *per* millilitre lysate (black diamonds). The concentration of ZAP-70-YFP was determined by FCS. Array-bound fluorescence of ZAP-70-YFP increased linearly over the concentration range tested. Binding of ZAP-70-YFP from a pervanadate treated lysate prepared at 10×10^6 cells *per* millilitre was strongly reduced (open diamond). (B) pITAM spots on arrays incubated with lysates of 1, 10 and 50×10^6 cells *per* millilitre displayed an increasing fluorescence intensity of ZAP-70-YFP, while indirect immunostaining against phosphotyrosine using a Cy5-labelled secondary antibody revealed that pITAM was not saturated by ZAP-70-YFP. (C) Western blot analysis of endogenous ZAP-70 from lysates of untransfected cells prepared at cell densities from 2 to 50×10^6 cells *per* millilitre. Equal volumes of lysate were loaded. Pervanadate treatment of the cells prior to lysis is denoted by pv. (D) ZAP-70 Western bands shown in (C) were quantitated by integrating their density and area. The ZAP-70 content increased linearly with the density of cells in the lysate. (E) Aliquots of the lysates depicted in (D) were incubated on arrays and the arrays indirectly immunostained for ZAP-70. A correlation between ZAP-70 content as determined by Western blotting and intensity of the immunostaining on the array was established for lysates of resting cells (black diamonds). An array incubated with lysate from pervanadate treated cells (open diamond) showed a clear reduction of immunostaining. Error bars represent the mean deviation from the mean.

Table 1. Pervanadate-dependent changes in the number of ZAP-70 molecules with unmasked SH2 domains *per* cell. Numbers given relate to ZAP-70-YFP for cells overexpressing the fusion protein and to endogenous ZAP-70 for untransfected cells

	ZAP-70-YFP with unmasked SH2 domains		Endogenous ZAP-70 with unmasked SH2 domains
	Concentration (nM)	Molecules per cell	Molecules *per* cell
Resting cells	19.9 ± 2.2[a)]	$(1.20 \pm 0.13) \times 10^6$	4.8×10^5[c)]
PV treated cells	7.1 ± 0.4[b)]	$(0.43 \pm 0.02) \times 10^6$	1.0×10^5[d)]

a) Directly determined by FCS
b) Calculated from array-bound fluorescence using the calibration curve of array-bound fluorescence *versus* ZAP-70-YFP concentration (Fig. 5A)
c) Estimated from the 2.5-fold overexpression of ZAP-70-YFP over endogenous ZAP-70 as determined by Western blotting (Fig. 4A)
d) Estimated from array-bound fluorescence using the calibration curve of indirect immunostaining for array-bound ZAP-70 *versus* integrated Western band (Fig. 5E)

fluorescence staining for endogenous ZAP-70 most likely was not due to saturation. Rather, the immunostaining of bound ZAP-70 had not reached equilibrium under the incubation conditions used. However, as long as incubation times are carefully controlled, antigen-antibody interactions can be used quantitatively in nonequilibrium assays [22]. Especially for protein-peptide interactions with lower affinity, dissociation of bound protein after removal of the cell lysate would preclude a prolonged incubation to reach equilibrium. Even though the interaction of ZAP-70 with the pITAM peptide is of rather high affinity, we intended to validate the method for conditions appropriate for interactions of lower affinity, therefore using short incubation times with primary and secondary antibody. The observed decrease in array-bound fluorescence for lysate from pervanadate treated cells corresponded to an 80% decrease of endogenous ZAP-70 with unmasked SH2 domains.

Finally, we combined the information obtained from (i) determining the concentration of ZAP-70-YFP in lysates of resting cells by FCS; (ii) the relative pervanadate-dependent reduction of free binding sites derived from the calibration curves; and (iii) the level of overexpression of fusion protein *versus* endogenous protein to calculate absolute numbers of available ZAP-70-YFP or ZAP-70 molecules *per* cell both in resting and in pervanadate treated cells (Table 1). The total number of available ZAP-70 molecules (ZAP-70-YFP and ZAP-70) in cells overexpressing the fusion protein could be determined experimentally by Western blot analysis and quantification of the overexpression level of the fusion protein.

4 Concluding remarks

The detection of the signalling-dependent masking of binding sites represents a valuable new protocol for the application of peptide microarrays in the analysis of cellular signalling processes. The protocol provides a significant shortcut to the detection of molecular interactions in comparison to established techniques such as co-immunoprecipitation. While the identity of the binding partner in the complex is not resolved, the parallel detection of binding events using microarrays functionalised with a multitude of peptides will provide a detailed description of the functional state of signalling proteins inside a cell. Given a repertoire of peptides that act as specific sensors for individual signalling proteins, each spot of a microarray may specifically report on the availability of a specific binding site.

In these multiplexed assays, cocktails of primary antibodies together with only one secondary antibody may be employed for the parallel detection of binding events. Multiplexed immunoassays for the quantitative detection of up to 20–30 analytes have been described (reviewed in [23]). With a similar number of protein-peptide interactions addressed in parallel, our concept may be employed to simultaneously probe the changes in the interaction state of multiple proteins engaging in cellular signalling. The affinity range of protein-peptide interactions detectable by this technique will have to be determined. Interactions will have to withstand multiple washing steps. Compared to other interactions of proteins with peptide motifs, the interaction of the ZAP-70 SH2 domains with the pITAM peptide is of rather high affinity. However, the applicability of peptide microarrays for the profiling of interactions with dissociation constants in the upper nanomolar to lower micromolar has already been demonstrated [8, 9].

In future experiments, similar to the assembly of collections of antibodies with optimised specificity, collections of peptides with optimal specificity for individual proteins need to be identified. Instead of peptide microarrays, protein microarrays may be used to monitor the masking of binding sites in a similar way. However, especially for interactions involving PTMs, different functional states of an interaction motif may be incorporated in peptide microarrays in a highly defined manner.

Finally, through acquisition of calibration curves, *e.g.*, by Western blot analysis, quantitative information on the fraction of a protein recruited into a molecular complex is obtained. If cells expressing a fusion protein with a fluorescent protein are available, combination of the microarray-based approach with FCS yields absolute figures on the change of available binding sites both in cells overexpressing the fusion protein and, through comparison of expression levels by Western blotting, also in cells only expressing the endogenous protein.

We thank Günther Jung for excellent facilities in peptide chemistry and instrumental analysis and Nicole Sessler for support in peptide synthesis. This work was supported by the German Science Council (DFG, Sonderforschungsbereich 510). K. K. is a scholar of the Graduiertenkolleg 794. R.B. gratefully acknowledges financial support from the Volkswagen Foundation "Nachwuchsgruppen an Universitäten".

5 References

[1] Brem, R. A., Yvert, G., Clinton, R., Kruglyak, L., *Science* 2002, *296*, 752–755.

[2] Cho, R. J., Huang, M., Campbell, M. J., Dong, H. *et al., Nat. Genet.* 2001, *27*, 48–54.

[3] Holstege, F. C. P., Jennings, E. G., Wyrick, J. J., Tong, I. L. *et al., Cell* 1998, *95*, 717–728.

[4] Niemeyer, C. M., Blohm, D., *Angew. Chemie. Int. Ed.* 1999, *38*, 2865–2869.

[5] Anderson, K., Potter, A., Baban, D., Davies, K. E., *Brain* 2003, *126*, 2052–2064.

[6] Nielsen, U. B., Cardone, M. H., Sinskey, A. J., MacBeath, G. *et al., Proc. Natl. Acad. Sci.USA* 2003, *100*, 9330–9335.

[7] Pawson, T., Nash, P., *Science* 2003, *300*, 445–452.

[8] Landgraf, C., Panni, S., Montecchi-Palazzi, L., Castagnoli, L. *et al., PLoS. Biol.* 2004, *2*, E14.

[9] Otte, L., Wiedemann, U., Schlegel, B., Pires, J. R. *et al., Protein Sci.* 2003, *12*, 491–500.

[10] Espejo, A., Cote, J., Bednarek, A., Richard, S. *et al., Biochem. J.* 2002, *367*, 697–702.

[11] Chan, A. C., Iwashima, M., Turck, C. W., Weiss, A., *Cell* 1992, *71*, 649–662.

[12] Sloan-Lancaster, J., Zhang, W., Presley, J., Williams, B. L. *et al., J. Exp. Med.* 1997, *186*, 1713–1724.

[13] Barber, E. K., Dasgupta, J. D., Schlossman, S. F., Trevillyan, J. M. *et al., Proc. Natl. Acad. Sci. USA* 1989, *86*, 3277–3281.

[14] Ottinger, E. A., Botfield, M. C., Shoelson, S. E., *J. Biol. Chem.* 1998, *273*, 729–735.

[15] Neumeister, E. N., Zhu, Y., Richard, S., Terhorst, C. *et al., Mol. Cell Biol.* 1995, *15*, 3171–3178.

[16] Elbs, M., Brock, R., *Anal. Chem.* 2003, *75*, 4793–4800.

[17] Laemmli, U. K., *Nature* 1970, *227*, 680–685.

[18] Schwille, P., Kummer, S., Heikal, A. A., Moerner, W. E. *et al., Proc. Natl. Acad. Sci. USA* 2000, *97*, 151–156.

[19] Exley, M., Varticovski, L., Peter, M., Sancho, J. *et al., J. Biol. Chem.* 1994, *269*, 15140–15146.

[20] Rigler, R., Mets, Ü., Widengren, J., Kask, P., *Eur. Biophys. J.* 1993, *22*, 169–175.

[21] Thompson, N. L., in: Lakowicz, J. R. (Ed.), *Topics in Fluorescence Spectroscopy*, Plenum, New York 1991, pp. 337–377.

[22] Schramm, W., Paek, S. H., *Anal. Biochem.* 1991, *196*, 326–336.

[23] Templin, M. F., Stoll, D., Bachmann, J., Joos, T., O., *Comb. Chem. High Throughput Screen.* 2004, *7*, 223–229.

